DEPARTMENT OF DEFENCE
DEFENCE SCIENCE & TECHNOLOGY ORGANISATION
DSTO

DSTO

Cold Expansion Tests for Plates Containing Elongated Holes

M. Heller, R. L. Evans and R. B. Allan

DSTO-TN-0233

Cold Expansion Tests for Plates Containing Elongated Holes

M. Heller, R. L. Evans and R. B. Allan

Airframes and Engines Division
Aeronautical and Maritime Research Laboratory

DSTO-TN-0233

ABSTRACT

Cold-expansion testing of D6ac plates containing an elongated (non-circular) hole, of 2:1 aspect ratio, has been undertaken using an AMRL designed interference fit plug/sleeve arrangement. The aim has been to determine the practical viability of the process as an option for addressing the cracking problem at the non-circular fuel flow vent hole number 13 in the wing pivot fitting of the F-111C aircraft in service with the RAAF. The key issue being that in the open literature, only cold expansion to circular holes has been reported, and application to non-circular holes would represent a significant new development. In the testing, three nominally identical plate specimens were cold expanded, with sleeves of two different material types (ie high strength tool steel (D2) and stainless steel) being assessed. Strain gauge readings around the elongated hole boundary were recorded at various stages of the cold-expansion process, as well as some typical full-field qualitative photoelastic strain distributions. In all cases nominal expansion levels greater than 2.5% were achieved, along with maximum peak strains of more than 10,000 micro-strain and maximum residual strains greater than 1600 micro-strain. These results indicate that highly effective cold expansion has been achieved. It was also demonstrated that subsequent to cold expansion, effective interference fitting could be achieved, without the need for post cold-expansion machining. The particular advantages available by using stainless steel sleeves have been identified, and an improved surface finish at the holes in the plug is also recommended. Fatigue testing of the existing design, (with minor amendments) is now proposed to confirm its anticipated suitability as an effective fatigue life extension option.

Published by

DSTO Aeronautical and Maritime Research Laboratory
PO Box 4331
Melbourne Victoria 3001 Australia

Telephone: (03) 9626 7000
Fax: (03) 9626 7999

AR-011-113
October 1999

APPROVED FOR PUBLIC RELEASE

Cold Expansion Tests for Plates Containing Elongated Holes

Executive Summary

An area of particular concern for the F-111C airframe in service with the RAAF is the wing pivot fitting in which there are a number of elongated (ie non-circular) machined fuel flow vent holes. For example, the region near fuel flow vent hole number 13 (FFVH13), is susceptible to fatigue cracking, and this problem could compromise the structural integrity of the F-111C fleet out to the planned withdrawal date of 2020. Currently, the problem is being managed by periodically reshaping the fuel flow vent holes to one of a family of progressively larger shapes, thereby removing any existing cracks. Unfortunately, this process does not completely eliminate further cracking, and at the current rate of crack growth and hole reshaping, the continued application of this method may not enable the aircraft to reach its desired service life.

In the present investigation cold-expansion testing of D6ac plates containing an elongated (non-circular) hole, of 2:1 aspect ratio, has been undertaken using an AMRL designed interference fit plug/sleeve arrangement. The aim has been to determine the practical viability of the process as an option for addressing the cracking problem at the non-circular fuel flow vent hole number 13 in the wing pivot fitting of the F-111C aircraft in service with the RAAF. The key issue being that in the open literature, only cold expansion to circular holes has been reported, and application to non-circular holes would represent a significant new development. In the testing, three nominally identical plate specimens were cold expanded, with sleeves of two different material types (ie high strength tool steel (D2) and stainless steel) being assessed. Strain gauge readings around the elongated hole boundary were recorded at various stages of the cold-expansion process, as well as some typical full-field qualitative photoelastic strain distributions. In all cases nominal expansion levels greater than 2.5% were achieved, along with maximum peak strains of more than 10,000 micro-strain and maximum residual strains greater than 1600 micro-strain. These results indicate that highly effective cold expansion has been achieved. It was also demonstrated that subsequent to cold expansion, effective interference fitting could be achieved, without the need for post cold-expansion machining. The particular advantages available by using stainless steel sleeves have been identified, and an improved surface finish at the holes in the plug is also recommended. Fatigue testing of the existing design, (with minor amendments) is now proposed to confirm its anticipated suitability as an effective fatigue life extension option.

Fatigue testing of the existing AMRL interference fit plug/sleeve design, (with minor amendments) is now recommended to confirm its anticipated suitability as an highly effective option for extending the fatigue life of the fuel flow vent hole number 13 region of the F-111C aircraft.

Authors

M. Heller
Airframes and Engines Division

Manfred Heller completed a B. Eng. (Hons.) in Aeronautical Engineering at the University of New South Wales in 1981. He was awarded a Department of Defence Postgraduate Cadetship in 1986, completing a PhD at Melbourne University in 1989. He commenced work in Structures Division at the Aeronautical Research Laboratory in 1982. He has an extensive publication record focussing on the areas of stress analysis, fracture mechanics, fatigue life extension methodologies and experimental validation. Since 1992 he has led tasks which develop and evaluate techniques for extending the fatigue life of ADF aircraft components and provide specialised structural mechanics support to the ADF. He is currently a Senior Research Scientist in AED and the Functional Head for Structural Mechanics.

R. L. Evans
Airframes and Engines Division

Rebecca Evans completed a Bachelor of Engineering in Aeronautical Engineering at the Royal Melbourne Institute of Technology in 1987. In 1988 she commenced work in Systems Division at DSTO Salisbury, where she worked on the design, analysis and testing of towed targets. Since 1992 she has been working in the Airframes and Engines Division where she has undertaken experimental and finite-element analyses of metallic aircraft components, evaluating various fatigue life enhancement techniques.

R. B. Allan
Airframes and Engines Division

Robert Allan completed a B.E. (Aeronautical) at R.M.I.T. in 1978. Since then he has worked in the areas of aircraft structural design, repair and manufacturing at major Australian and U.S. aircraft companies. Some major projects worked on in this time were the tailplane and elevator design of the Wamira aircraft project, F-18 aft fuselage redesign and the support of local manufacture of numerous aircraft components. Prior to joining AMRL in 1994, he spent 5 years in the field of polymer flow characterisation and simulation using finite element methods. Since joining AMRL he has worked in the area of life extension through the use of structural mechanics in support of Australian Defence Force aircraft, specialising in finite element stress analysis and advanced experimental stress analysis.

Contents

Notation

b	bottom region for location of strain gauges
mm	Millimetres
Nm	Newton metre
r	Circular radius at end of elongated hole
t	top region for location of strain gauges
με	micro strain
θ	angular position
α	angular position

List of Abbreviations

AMRL	Aeronautical and Maritime Research Laboratory
CPLT	cold proof load test (The F-111C airframe is subjected to this static proof loading periodically to determine its damage tolerance)
DADTA	durability and damage tolerance analysis
FFVH	fuel flow vent hole
FFVH13	fuel flow vent hole number 13
RAAF	Royal Australian Air Force

1. Introduction

An area of major concern for the F-111C airframe, currently in service with the RAAF, is the wing-pivot fitting manufactured from D6ac steel. It contains a number of machined elongated (ie non-circular) fuel flow vent holes (FFVH), as shown in Figure 1. Under cold proof load tests (CPLT) the material around hole number 13 (i.e. FFVH13) experiences extensive plastic deformation, which results in the introduction of tensile residual stresses. These residual stresses, coupled with the local material response due to the remote loading sequence experienced in service, are detrimental and contribute to crack initiation and growth at this region. This problem could compromise the structural integrity of these aircraft out to the planned withdrawal date of 2020.

Currently, the problem is being managed by reshaping FFVH13 to one of a family of progressively larger shapes [1], and thereby removing any existing cracks. The extent of the rework depends on the size of the detected crack. For example, Figure 2 shows the original geometry for FFVH13 as well as two typical rework shapes. Unfortunately the reworking procedure does not completely eliminate further cracking, and at the current rate of crack growth and the reworking frequency, this method may not be sufficient to enable the F-111C to reach its desired service life. Recently a durability and damage tolerance analysis (DADTA) has been undertaken by Lockheed Martin to determine recommended inspection intervals based on the stress levels associated with the rework shapes. Their results indicate that unacceptably short inspection intervals are required [2, 3]. AMRL is presently reviewing the DADTA results with particular attention being given to assessing the level of conservatism in the analysis assumptions, and the degree of correlation with in-service crack growth data. If the reworking procedure cannot allow the aircraft to reach the desired service life, an alternative method of life extension will be required. In view of this problem, AMRL has been tasked with the development of a proposed non-circular cold-expansion/interference-fit plug option, for the life extension of FFVH13, with the aim of eliminating crack growth or significantly reducing the crack growth rate. It should be noted that cold expansion is currently being used for the life extension of circular bolt holes in the Overwing Longerons (of D6ac material) for the RAAF F-111 aircraft, [3]. Hence the application to non-circular holes would constitute a significant new development. The first requirement of such a non-circular cold-expansion/interference-fit plug option, is that the FFVH13 be accurately cut to a size similar to the maximum AMRL rework shape as shown in Figure 2. This would allow the repair to be applied to most holes in the fleet, irrespective of their current shape. The ability to cut such a hole, with a high degree of accuracy, has been demonstrated on an actual F-111 wing in prior work at AMRL. Here an advanced electro-discharge machining procedure was used, [4]. The second requirement is that the non-circular hole can be satisfactorily cold expanded and/or interference fitted.

The typical benefit of cold expansion and/or interference fitting for the life extension of plates containing circular holes is reasonably well established and documented. The use of interference fitting and/or cold expansion has been reviewed by Mann and Jost [5]. Closed form theoretical solutions only apply to the simplest configurations; thus finite-element analyses are typically employed to solve problems of practical importance. However, previous work in the literature does not give clear guidelines for either: (i) non-circular geometries, or (ii) complex remote-loading conditions and realistic strain-hardening material properties. Both of these issues need to be addressed when developing a life-extension option for the FFVH13 on the F-111C aircraft. Recent work by Allan and Heller [6] has however used two-dimensional finite-element analyses to investigate the second issue for an enhanced circular hole to gain a preliminary understanding of the interaction of the key parameters involved. This was followed by an investigation [7, 8], based on two-dimensional finite-element analyses, to quantify the effect on critical plate stresses due to the enhancement of a *non-circular* hole by combined cold expansion and interference fitting. This prior theoretical work indicted that enhancement through combined cold expansion and interference fitting should be considerably better than interference fitting alone. Also in this work, plate stress distributions measured experimentally due to *elastic interference fitting* to a level of approximately 0.74%, compared well with the finite element predictions. This demonstrated the suitability of a proposed tapered plug/sleeve design to achieve effective *elastic interference fitting* of an elongated hole. However, no cold-expansion testing, which typically requires approximately 1.5% or greater expansion, was undertaken.

Hence in this present investigation, the cold-expansion testing of a D6ac plate with an elongated (non-circular) hole has been undertaken with the aim of determining the practical viability of the process. A slightly modified version of an interference-fit tapered plug/sleeve design (essentially longer plug and backing plate, and minor drawing enhancements) which has recently been developed at AMRL [7, 8], was used. The experimental methods used in the investigation are presented in Section 2. In Sections 3 to 5 the results of cold-expansion tests on three nominally identical specimens are given. Here strain gauge results around the elongated-hole boundary are given at various stages of the cold-expansion process as well as some typical full-field qualitative photoelastic-strain distributions. A summary comparing strain-gauge results for the three specimens is then given in Section 6. This is followed by conclusions in Section 7.

2. Experimental Methods

Cold-expansion testing of three plate specimens (all nominally identical) was undertaken with two main aims. Firstly, it is desired to assess the practical viability of the non-circular interference-fit plug design to cold expand the plate material surrounding the elongated hole. The second aim was to obtain strain measurements at

locations around the elongated hole boundary (close to the hole edge) at various stages of the cold-expansion process.

2.1 Specimen Geometry

The geometry of the plate specimen containing an elongated hole, part number SE5/52/14/RS009-001, is shown in Figure 3. The plate is manufactured from D6ac steel and hardened to the same condition as the F111 wing-pivot fitting region. It is nominally 76 mm wide, 266 mm long and has a thickness of 5 mm. The hole has an aspect ratio of 2:1, being 50.8 mm long and 25.4 mm wide and its major axis is oriented at an angle of 16 degrees relative to the remote loading axis. This orientation for the hole was chosen to locate the maximum hoop stress (at the hole edge), in the same position as determined for an actual representative geometry and loading of the FFVH13 in the wing-pivot fitting, [1]. This geometry (with a slightly different plate length; 245 mm compared to 266 mm) was used in the experimental and two-dimensional finite-element work reported in [7].

2.2 Cold Expansion and Interference Fitting Method

The plug/sleeve design that was used to achieve cold expansion of the elongated hole is shown schematically in Figure 4, with a photograph of the key components given in Figure 5. The most recent engineering drawing of the components is given in Figure 6. It should be noted that for these experiments the plug was manufactured from a drawing without a surface finish specified for the hole bores. The repair concept involves initially placing a neat-fitting sleeve into an accurately machined elongated hole. The sleeve has a 1:50 taper on its internal surface that mates with a plug having the same taper on its outer surface. The plug is pulled into the sleeve by tightening two bolts. For these demonstration tests, M12 Unbrako high tensile bolts and nuts were used. The sleeve has a split mid way along one of its flat sides so that expansion is not unduly restricted during the insertion process. For all cold-expansion tests, the tapered plug manufactured from either D2 tool steel or stainless steel, (part number SE5/52/14/RS109-003) was used as indicated in Figure 6. The overall design of the arrangement offers a number of useful features including: (i) ease of removal for inspection of the hole when required, (ii) capacity for a variable expansion level, depending on the plug insertion depth, and (iii) possibility of varying the relative material properties of the sleeve and plug, as required. Clearly, filling the FFVH13 with an interference-fit repair will stop fuel flow, but this of no consequence since there are many other non-critical fuel flow holes in the wing-pivot fitting. In fact, more recent models of the F-111 aircraft have no hole at the FFVH13 location.

During the cold-expansion process one end of the specimen was clamped in the jaws of a machine vice. Initially the sleeve and plug were placed in the hole and the bolts hand tightened. Further tightening was then achieved using a torque wrench with the aim of keeping the bolt torques equal during the insertion process. Removal of the plug was achieved by reversing the backing plate (i.e. locating it on the front of the specimen)

and tightening the bolts onto two spacers. Before the insertion process was begun, the threaded portion of the bolts and the outside of the plug were lubricated with G-n Dow Corning grease. The level of interference achieved can be readily estimated from the plug insertion distance, knowing that the taper ratio of the outside of the plug was 1:50. Hence the distance the plug needs to be inserted into the sleeve/plate to achieve a nominal 1% radial interference is 6.35 mm. For all tests the nominal degree of cold expansion, based on the initial radius at the end of the hole and the initial plug geometry, was between 2 and 3.5%.

2.3 Strain Measurements

Strain gauges were bonded to each of the three plate specimens (numbers 1, 2 and 3) around the perimeter of the hole at the locations shown in Figures 7, 8 and 9, respectively. For these locations the definition for the angular position of the gauges is given in Figure 10. The strain gauges used were Micro-Measurements type EA-06-050AH-120, which had a gauge length of 1.27 mm and a grid width of 1.02 mm. Strains were recorded during the cold-expansion process at intervals corresponding to increments in bolt torque of approximately 5 Nm.

Photoelastic coatings were also applied to each specimen to enable a qualitative photographic record of the full-field peak and/or residual strain fields to be made. Initially for Specimen 1, photoelastic coatings of four different thickness were applied as shown in Figure 11, with further details given in Table 1. The different thickness coatings were used to determine the best choice for the testing of the subsequent specimens, noting that each thickness had a different sensitivity to strain. The photoelastic sheets were type PS-1 from Micro-Measurements Group. The type PC-8 adhesive was used, also from Micro-Measurements Group, since it was suited to high strain studies where elongation can exceed 3 %. For all photoelastic measurements the coating was illuminated with a 75 W, 12 volt halogen light passing through a Budd Large Field Universal Meter (polariscope) with one layer of circular-polariser filter. The resulting strain field was viewed and photographed through one layer of polaroid HN32 circular-polariser filter, of 0.762 mm (0. 0.030") thickness. Photographs were taken with a SLR camera using 100 ASA daylight colour film. Based on the results obtained for the first specimen, the 2 mm thick photoelastic coating was selected for the testing of Specimens 2 and 3.

During the plug insertion process the assembly length, as defined in Figure 4, was recorded as well as the strain-gauge measurements. From this information the amount of plug insertion distance was determined to achieve a given strain response. The nominal plug insertion values then needed to be corrected (by a small constant offset) to allow for the initial 'settling in' of the plug; ideally full contact between the plug and the sleeve/plate exists. Here the 'raw' strains versus plug displacement responses for each gauge were extrapolated to zero, and a zero value of *plug displacement* determined. For future reference the bolt torque used during the insertion process was also recorded for Specimens 1 and 2 and is plotted in Figure 12.

3. Testing of Specimen 1

3.1 Cold Expansion

For the testing of Specimen 1 (serial number FF8AL), a sleeve (part number SE5/52/14/RS109-002) manufactured from D2 tool steel, was used. The strain-gauge data obtained during this test is listed in Tables 2 and 3 as a function of plug assembly length and plug displacement, and is also plotted in Figure 13. The peak strains for each strain gauge are presented in Table 4, along with the residual strains after the plug and sleeve have been removed. It can be seen that tensile hoop strains up to 24,000 με occur at particular locations in the curved regions, while the radial strains are compressive along the flat sides. It is clearly demonstrated by the magnitude of the residual strains (of up to 13150 με) that highly effective cold expansion (ie residual plastic deformation) has been achieved, noting that the yield strain for D6ac steel is approximately 6500 με. The plotted strain given in Figure 13 also indicate that the strain response is not smooth at some gauge locations. The photoelastic results obtained at the maximum cold-expansion level are presented in Figure 14, and show that the main effect of cold expansion occurs at the end radii of the hole. Based on these photoelastic results the 2 mm thick material was considered the most desirable in terms of clarity, since it developed around five fringes (red-blue transitions) for the cold-expansion removal case. The maximum nominal cold-expansion level was calculated to be 2.78% based on corrected plug displacement and the original geometry.

During the cold-expansion procedure, marked cracking sounds were heard during both plug insertion and removal. This was believed to be due to cracking of the sleeve and/or plug. Upon completion of the test it was found that the sleeve had split radially in five places as shown in Figure 15. Here it should be noted that the top, middle slit was the pre-exiting machined split in the sleeve. Additional circumferential cracking also existed around the inside of the sleeve, extending through the thickness at the lefthand end as shown in Figure 15. The plug also experienced some cracking, however it was still intact. As there were no replacement plugs the same plug was used in the cold-expansion testing of Specimens 2 and 3.

3.2 Subsequent Interference Fitting

Subsequent to the cold-expansion test it was decided to insert an interference-fit plug/sleeve assembly into the cold-expanded hole. For this stage of testing the four existing photoelastic coatings were replaced with a single thickness coating of 2 mm. The interference-fit arrangement is very similar to the cold-expansion assembly except for the length of the plug and the backing plate, as shown in the engineering drawing given in Figure 16. Also a new stainless steel sleeve was used. To be consistent with the new photoelastic measurements, the strain gauges were initialised to zero at the beginning of the test. The strain-gauge results in presented in this section are therefore

due to interference fitting only. The strain-gauge data are presented in Tables 5 and 6 as a function of plug assembly length and plug displacement, and are plotted in Figure 17. The peak strains for each strain gauge at the maximum interference level are presented in Table 7. The maximum nominal level of interference was calculated to be 1.26% based on plug displacement and original geometry. The maximum strains achieved were 3099 με at gauge 11 (hoop orientation and 157.5° angular position) and -3387 με at gauge 14 (radial orientation and 45° angular position). The full field photoelastic results given in Figure 18 show that an even interference-fit pattern has been established despite the level of prior cold working. This test confirmed that an interference fit could be achieved for the elongated hole which had already been cold expanded, and that reaming of the hole subsequent to cold expansion was not required. However, the over-sizing of the hole by approximately 0.034 mm (caused by the cold-expansion process) obviously needs to be taken into account when installing an interference-fit plug after cold expansion if a prescribed expansion level is to be achieved.

4. Testing of Specimen 2

For the testing of Specimen 2, (serial number EM47AG1A) the sleeve (part number SE5/52/14/RS109-002) was manufactured from stainless steel. One objective of this test was to ensure that a stainless steel sleeve would produce a significant level of cold-expansion strain, as was the case for the D2 sleeve. The strain gauge data is presented in Table 8 as a function of plug assembly length and plug displacement, and are plotted in Figure 19. The peak strains for each strain gauge at maximum cold-expansion level are presented in Table 9, along with the residual strains of the plate after the plug and sleeve have been removed. It can be seen that at the maximum cold-expansion level, tensile strains of up to 10294 με are achieved the curved regions, while the radial strains are compressive along the flat sides. It is clearly demonstrated by the maximum residual strain of 2019 με that effective cold expansion has been achieved. Inspection of the results plotted in Figure 19 show that the strain response is quite smooth at all strain-gauge locations. The maximum nominal cold-expansion level was calculated to be 2.16% based on corrected plug displacement.

The photoelastic results are presented in Figure 20 for following two loading conditions, (i) at maximum cold expansion (left), and (ii) after the removal of the cold-expansion plug and sleeve (right). Since the photoelastic coating was damaged during the removal process, some anomalous fringe patterns along the flat sides of the hole are evident. However, it is clear that the strain distribution at maximum cold expansion level has been fully developed and is comparable to that obtained for Specimen 1 with the D2 sleeve. A well formed residual strain field around the end radii of the hole is also shown to exist after the cold-expansion process. Examination of the sleeve after cold expansion showed the presence of small cracks, as given in Figure 21. On removal

the plug broke into two pieces, however this did not seem to be a problem during the cold-expansion process, since the plug is essentially held together by compressive forces around its outside boundary.

5. Testing of Specimen 3

For the testing of Specimen 3, (serial number EM52AA2A) the stainless-steel sleeve (part number SE5/52/14/RS109-002) and the same (ie damaged) plug from the previous tests were used. This test was essentially a repeat of the test on Specimen 2. The strain-gauge data is presented in Table 10 as a function of plug assembly length and plug displacement, and are also plotted in Figure 22. The peak strains for each strain gauge at maximum cold-expansion level are presented in Table 11, along with the residual strains after the plug and sleeve have been removed. It can be seen that at the maximum cold-expansion level, tensile hoop strains up to 13,539 με occur in the curved regions, while the radial strain is compressive along the flat sides. It is demonstrated by the residual strains (of up to 3236 με) that effective cold expansion has been achieved. Inspection of the results plotted in Figure 22, also show that the strain response is not smooth at some strain-gauge locations. The maximum nominal cold-expansion level was calculated to be 3.49% based on plug displacement and the original geometry.

The photoelastic results are presented in Figure 23 for the maximum cold-expansion case (left), and after the removal of the cold-expansion plug and sleeve (right). The result at maximum cold-expansion shows the strain distribution has been fully developed and is comparable to that for Specimen 1 for the D2 sleeve. An even residual strain field around the end radii of the hole is shown to exist after the plug removal. The sleeve had a similar degree of cracking as occurred for Specimen 2, which may have been due to the damaged plug.

6. Summary of Results and Discussion

6.1 Strain Measurements

In the previous Sections 3, 4 and 5, the hoop and radial strain responses at all strain gauge locations have been presented in detail for each of the three specimen tests. In this section selected results at common locations for the three specimens are presented for convenience. A comparison of peak-strain results for the specimens obtained during the cold-expansion process is given in Table 12. It can be seen that in all three cases a maximum peak strain of greater that 10,000 με was achieved. Also, for gauges at the same locations there was good consistency between Specimens 2 and 3. This is pleasing since they both used the same type of sleeve material. In the curved region the strains for Specimen 1 were significantly higher than those for the other two specimens. This behaviour is expected since a harder and less ductile sleeve was used

for the first specimen, however it may also be due to the fact that a fractured plug was used for specimens 2 and 3. In Table 13 a comparison of residual-strain results obtained at the completion of the cold-expansion process is given. The tensile residual strains for Specimen 1 are much higher than those of Specimens 2 and 3 (ie a range of 5000 to 13150 με, as compared 1000 to 3236 με). This is consistent with the relative level of peak strains achieved for the different specimens.

6.2 Cracking of the Plug Due to Cold Expansion

During the first cold-expansion test, the plug fractured as shown in Figure 24. The plug was still intact and as there were no replacement plugs, the same plug was used in all subsequent cold-expansion testing. During the second cold-expansion test the plug cracked all the way through as shown in Figure 25. The effect of the plug being in two pieces can be seen from the strain data for Specimens 2 and 3. After the cracked plug was used in Specimen 2, permanent deflection of the plug ends at the crack meant that the strain rate per insertion distance dropped, but was made up as the permanent deflection point was passed. Nevertheless, the plug was still effective in producing very high strains in the plate, since during the cold expansion process the plug is essentially subjected to compressive forces around its outside boundary. Examination of the fracture surfaces of the plug indicated that cracking initiated at two locations at the edge of the holes, and then spread leading to complete splitting of the plug. Inspection of the plug hole bores, (which were manufactured to a drawing which erroneously had no surface finish specified), revealed scoring due to the boring process. Thus the cracks initiated at these stress concentrations. It is also believed that the use of the very hard D2 sleeve could have contributed to the plug cracking. Hence for any future testing, it is recommended that the more ductile stainless steel sleeves are used. It is also recommended that the hole bores of the tapered plug have a surface finish of N6, as is denoted in the most recent engineering drawing given in Figure 6.

7. Conclusions

The AMRL interference fit plug/sleeve design has been shown to be highly effective for achieving extensive cold expansion of a D6ac plate containing an elongated (ie non-circular) hole, with an aspect ratio of 2:1. Three nominally identical specimens were cold expanded, with sleeves of two different material types (ie high strength tool steel (D2) and stainless steel) being trialled. In all cases nominal expansion levels greater than 2.5% were achieved along with maximum peak strains of more than 10,000 micro-strain and maximum residual strains greater than 1600 micro-strain.

It was also demonstrated that effective interference fitting could be achieved for the elongated hole, which had already been cold expanded, without the need for post cold-expansion machining. The particular advantages available by using the stainless steel

sleeves have been identified, in that they were not significantly damaged during the expansion process, whereas the D2 sleeve was susceptible to cracking. Cracking of the plug was also evident and this was attributed primarily to the poor surface finish at the bore holes in the plug. Hence in future it is recommended that these holes are manufactured with an improved surface finish.

Fatigue testing of the existing design, (with minor amendments) is now recommended to confirm the expected suitability of this design as a fatigue life extension option for elongated holes, such as the critical fuel flow holes in the wing pivot fitting of the F-111C airframe.

8. Acknowledgments

The authors wish to thank Mr P. Piperias and Mr K. Lemm for their contributions to the interference fit plug/sleeve assembly design, and Mr N. Absolom for his technical assistance with the experimental work. The authors also wish to acknowledge the helpful comments and suggestions given by Mr K. C. Watters, Dr L. F. R. Rose and Mr N. Goldsmith.

9. References

1. **KEYS, R.H., MOLENT, L., and GRAHAM, A.D.,** *F-111 wing pivot fitting finite element analysis of rework of fuel flow vent hole #13,* DSTO, ARL, Aircraft Structures Technical Memorandum 557, 1992.

2. **ANON.,** *RAAF F-111C Durability and Damage Tolerance Analysis Results,* Lockheed Martin Report FZS-12-5034, 15 September 1998.

3. **ANON.,** *Final report on phase II for D6ac bolt hole life improvement - F-111 coldwork modification development program.,* General Dynamics Report, FZS-12-588, 10 April 1991.

4. **WALKER, K.,** *Improved electrical discharge machining procedures for re-work of fuel flow vent hole No. 13 in F-111 wing pivot fitting,* AMRL, Structures Laboratory Report No. 9/96, September 1996.

5. **MANN, J.Y., and JOST, G.S.,** *Stress fields associated with interference fitted and cold-expanded holes, with particular reference to the fatigue life enhancement of aircraft structural joints,* Metals Forum, Vol. 6, No. 1. 1983.

6. **ALLAN, R.B. and HELLER, M.,** *Stress analysis of a plate containing a round hole with combined cold expansion and interference fitting under F-111C representative loading conditions,* DSTO, AMRL, Technical Report DSTO-TR-0523, April 1997.

7. **ALLAN, R. B., and HELLER, M.,** *Stress analysis of an interference fit life extension option for a cold expanded elongated fuel flow hole on the F-111C aircraft,* DSTO, AMRL, Technical Report DSTO-TR-0549, June 1997.

8. **HELLER, M., ALLAN, R. B., and PIPERIAS P.,** *Stress analysis of an interference fit repair option for fuel flow vent hole 13 on the F-111C aircraft,* Proceedings of the First Australian Congress on Applied Mechanics, Melbourne, 21-23 February 1996, Vol. 1 pp. 151-158, 1996.

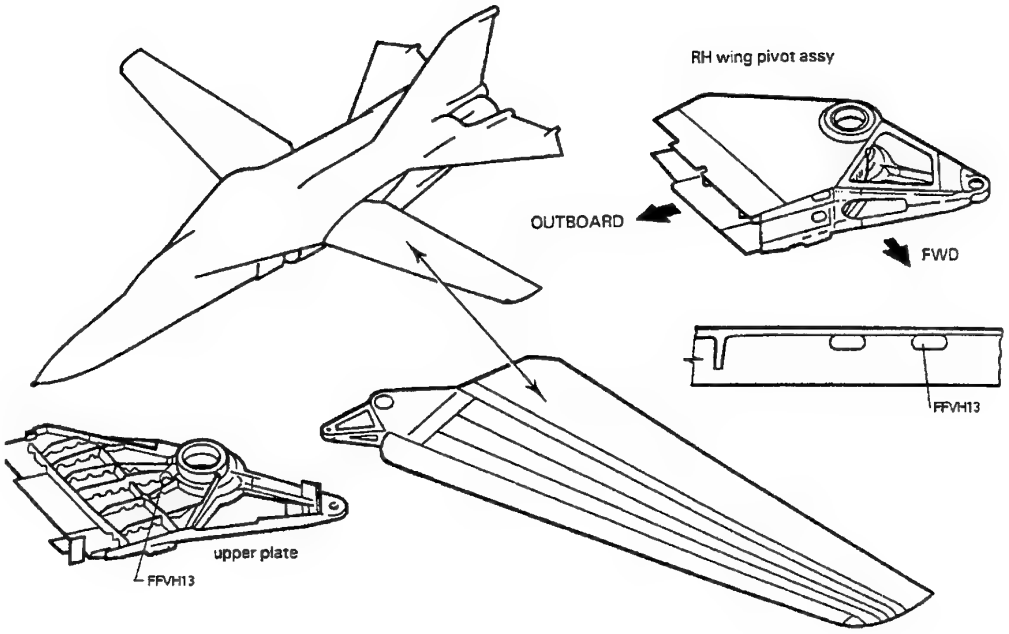

Figure 1. F-111 aircraft and wing showing the location of fuel flow vent hole number 13 (FFVH13) in the wing pivot fitting.

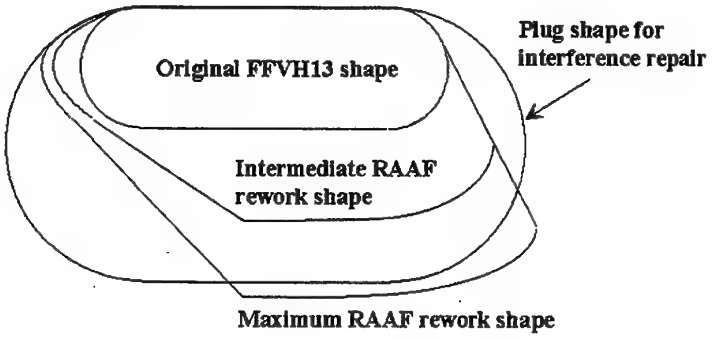

Figure 2. Comparison of the original geometry of FFVH13 with typical RAAF rework shapes and proposed hole for interference-fit plug.

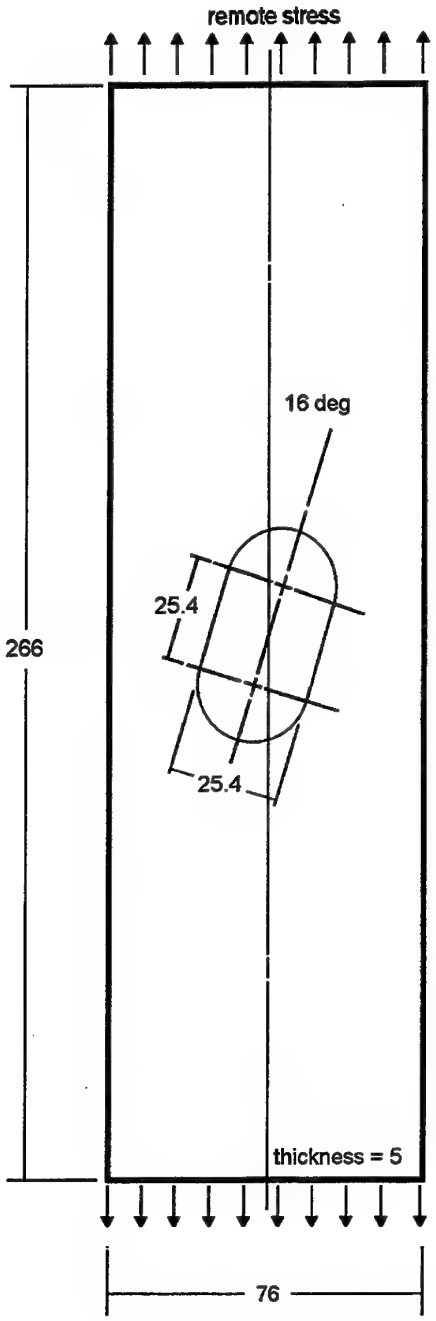

Figure 3. Nominal geometry of test specimen plates.

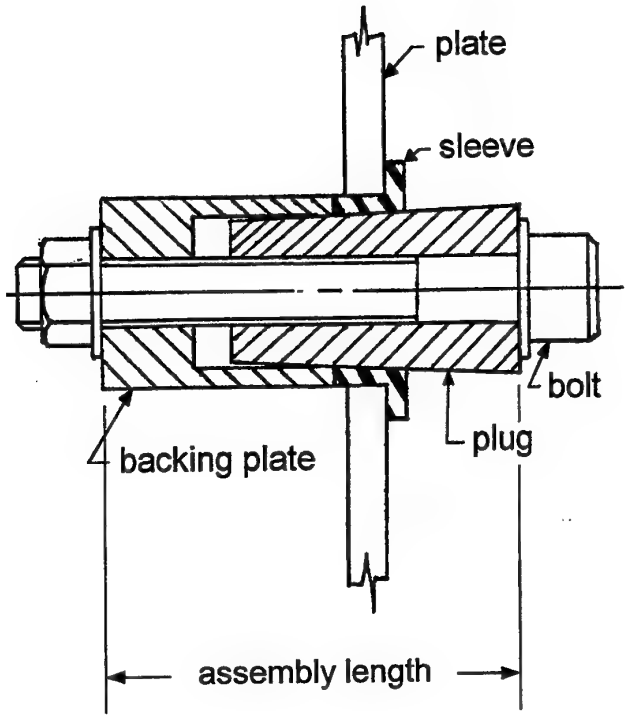

Figure 4. Schematic of the cold-expansion plug/sleeve design inserted into a plate with an elongated hole.

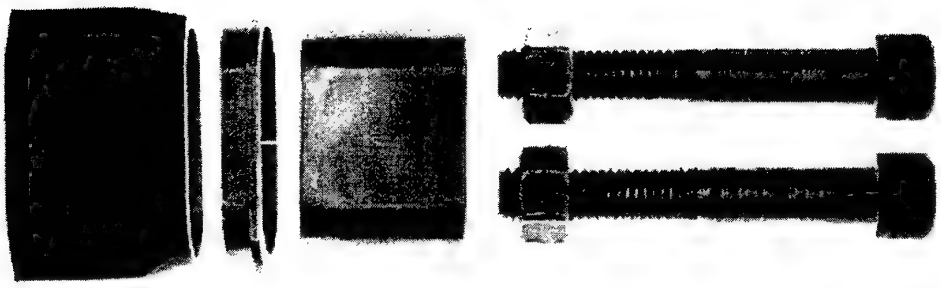

Figure 5. Photograph of key components for the interference-fit plug assembly, showing from left to right; backing plate, tapered sleeve, tapered plug and bolts.

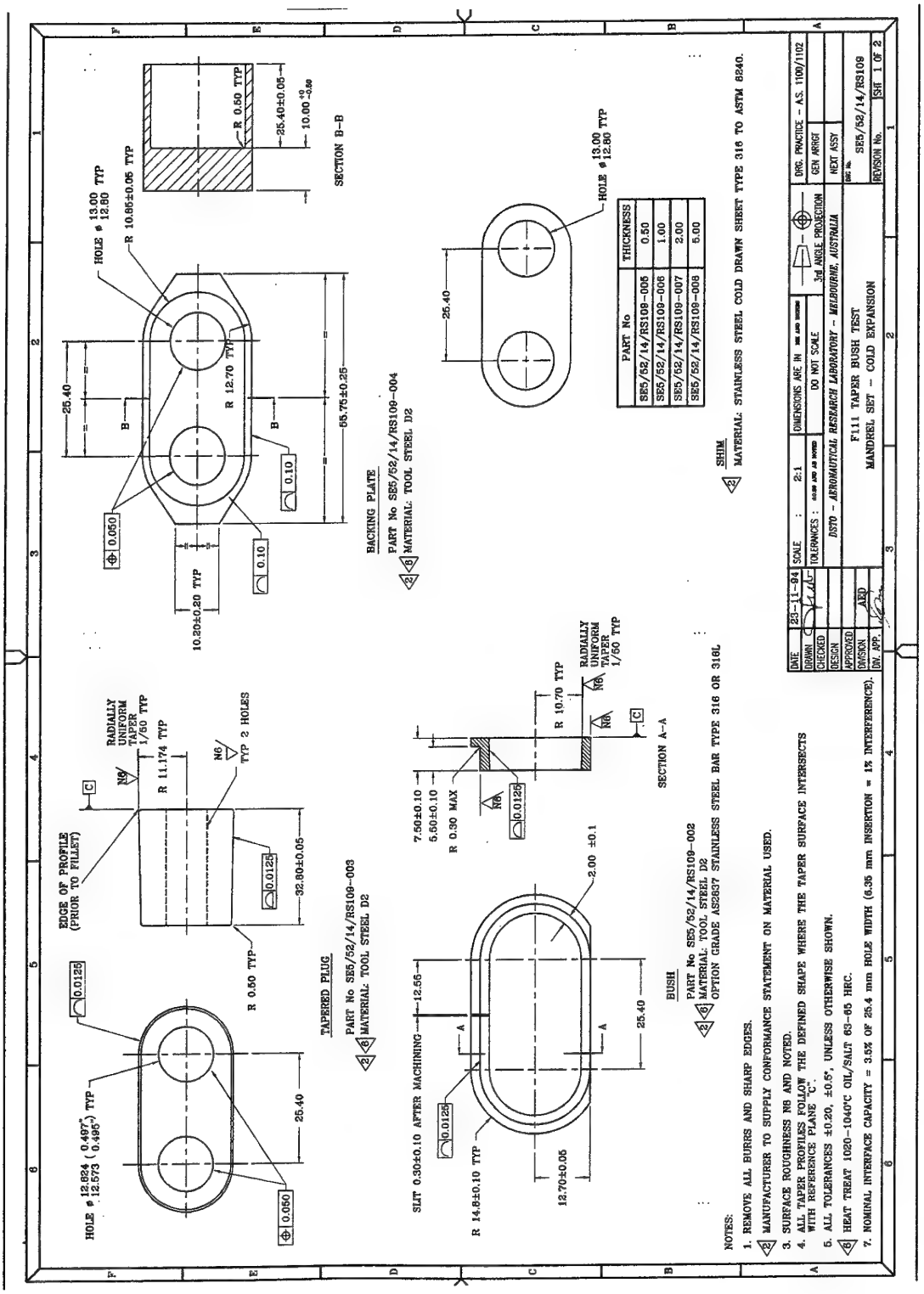

Figure 6. Engineering drawing of components comprising assembly for cold expansion.

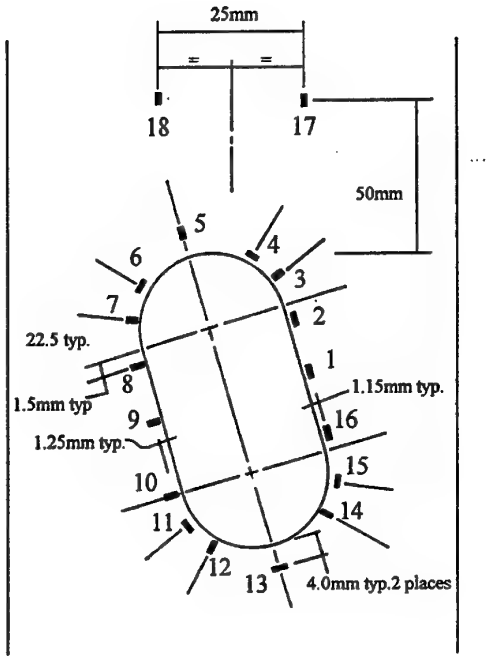

Figure 7. Orientation and location of strain gauges around hole boundary on back face of Specimen 1.

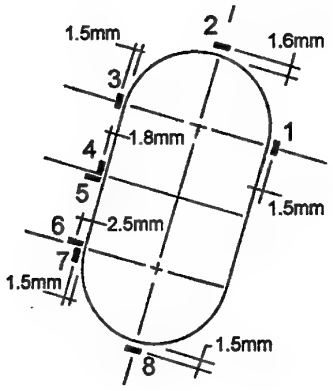

Figure 8. Orientation and location of strain gauges around hole boundary on front face of Specimen 2.

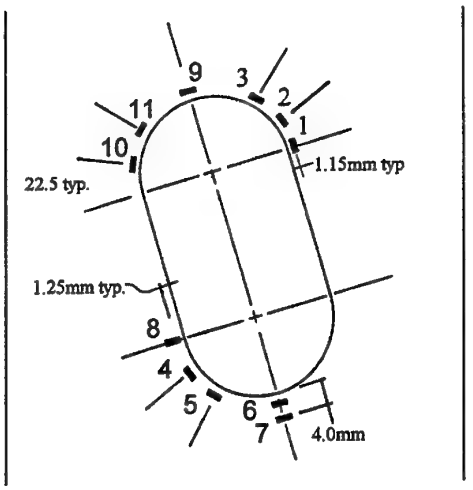

Figure 9. Orientation and location of strain gauges around hole boundary on back face of Specimen 3.

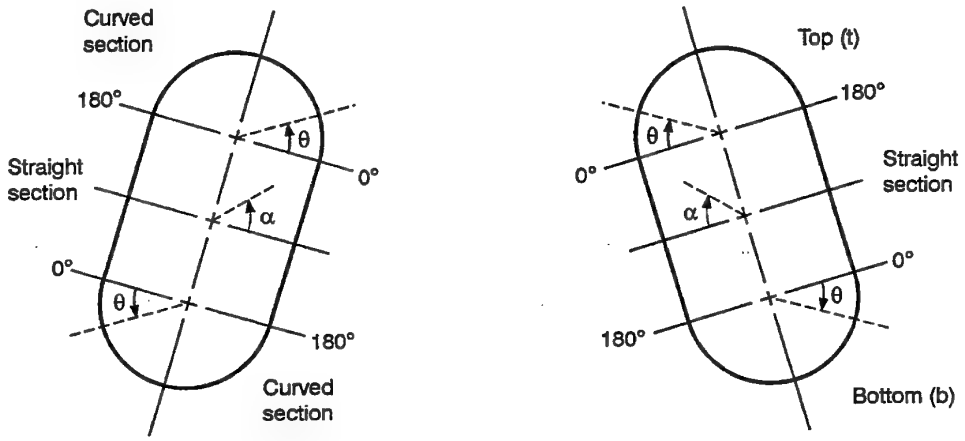

Figure 10. Geometry for definition of position around hole boundary for strain-gauges on front face of specimen (left) and back face of specimen (right).

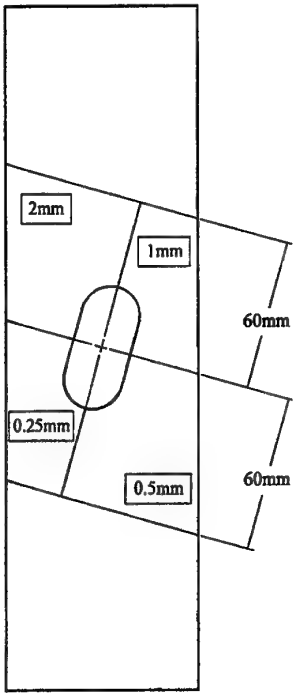

Figure 11. Location and thicknesses of photoelastic coatings on Specimen 1.

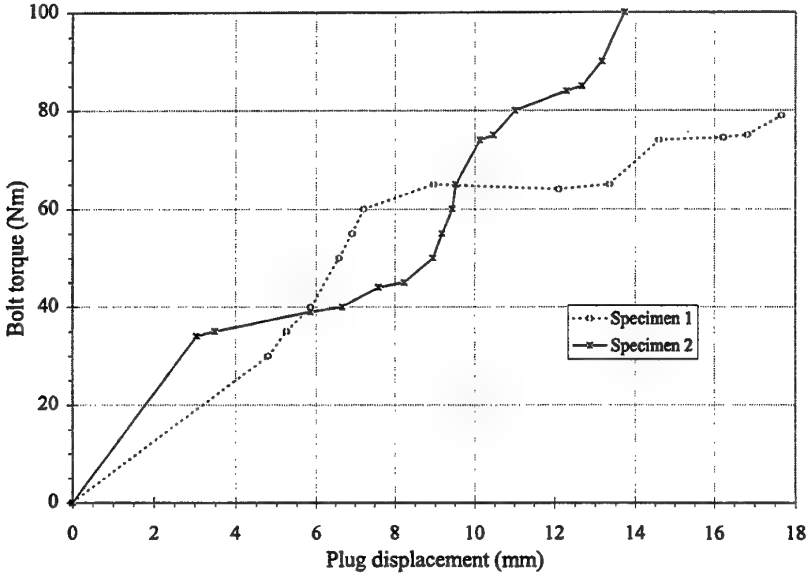

Figure 12. Bolt torque versus plug displacement during the cold-expansion process for Specimens 1 and 2 (values not recorded below 30Nm).

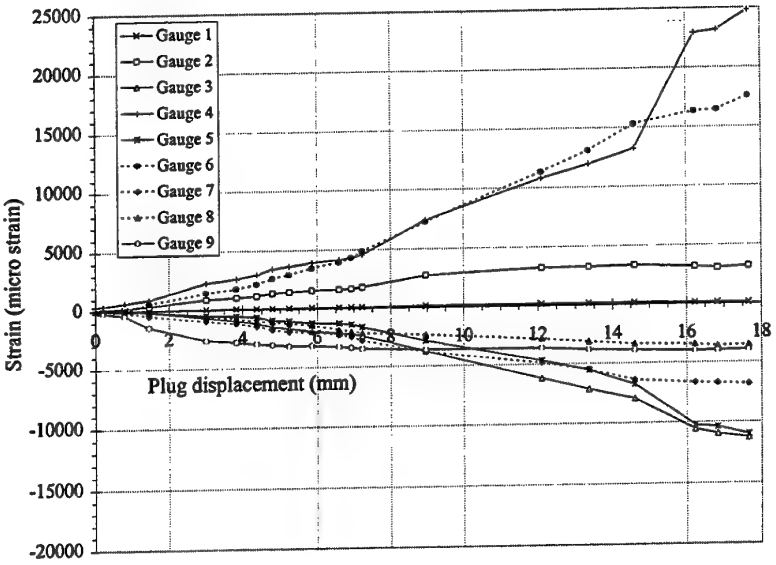

(a) Strain gauges 1 to 9

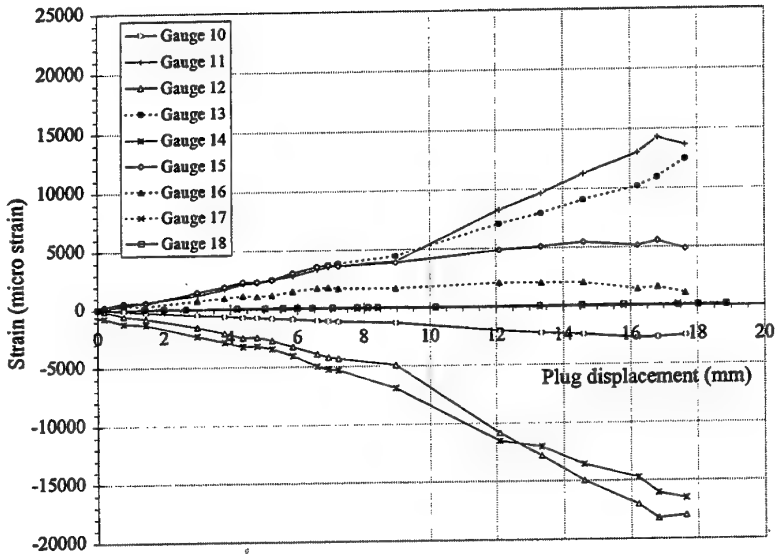

(b) Strain gauges 10 to 18

Figure 13. Strain response as a function of corrected plug displacement for Specimen 1, during the cold-expansion process.

Figure 14. Photoelastic strain distribution at the maximum cold-expansion level for Specimen 1.

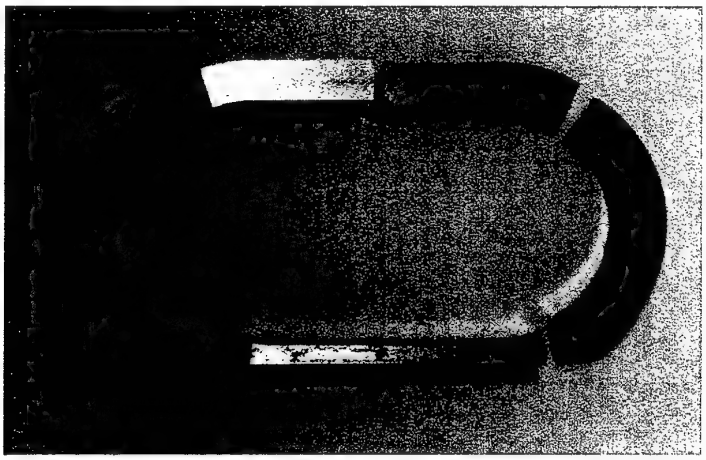

Figure 15. D2 sleeve of Specimen 1 after cold-expansion test completion, showing multiple fractures (original manufactured slit is at top centre).

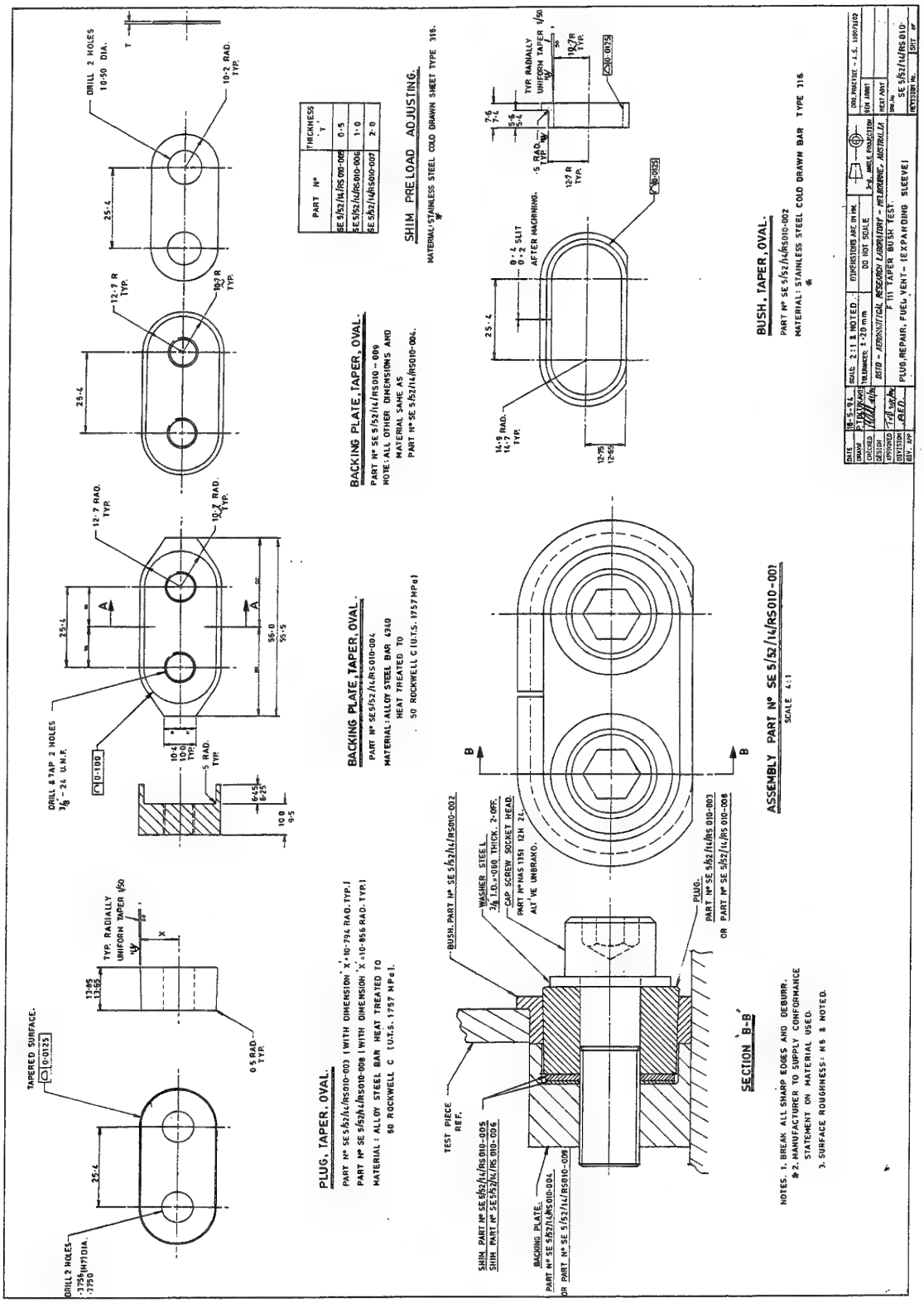

Figure 16. Engineering drawing of components comprising assembly for interference fitting.

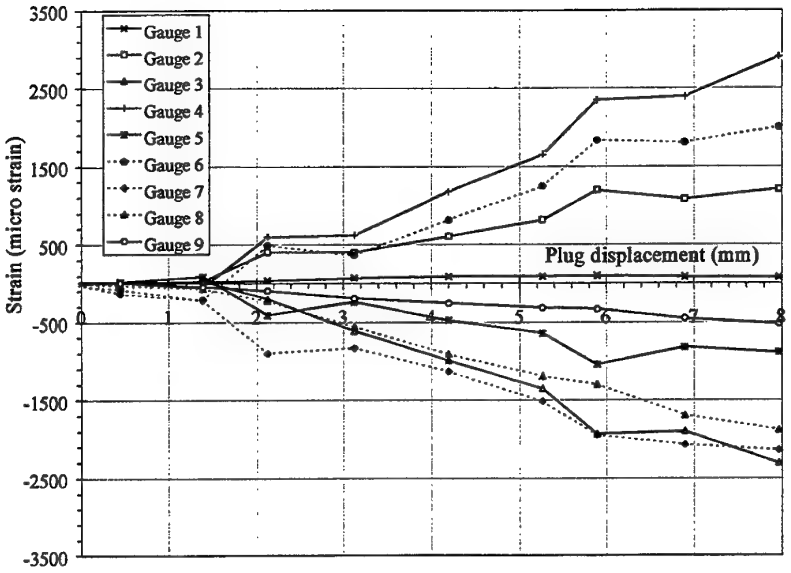

(a) Strain gauges 1 to 9

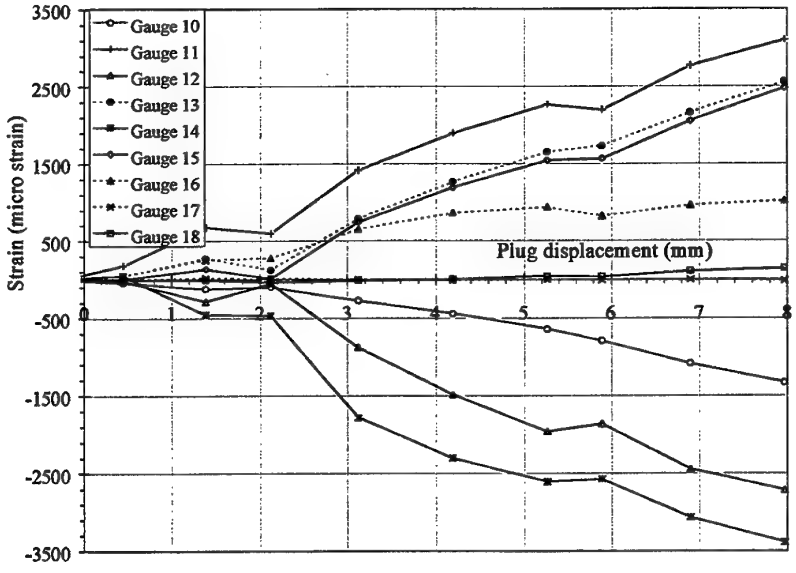

(b) Strain gauges 10 to 18

Figure 17. Strain response as a function of plug assembly length for Specimen 1, during the interference-fitting process (gauges 'zeroed' before test commencement).

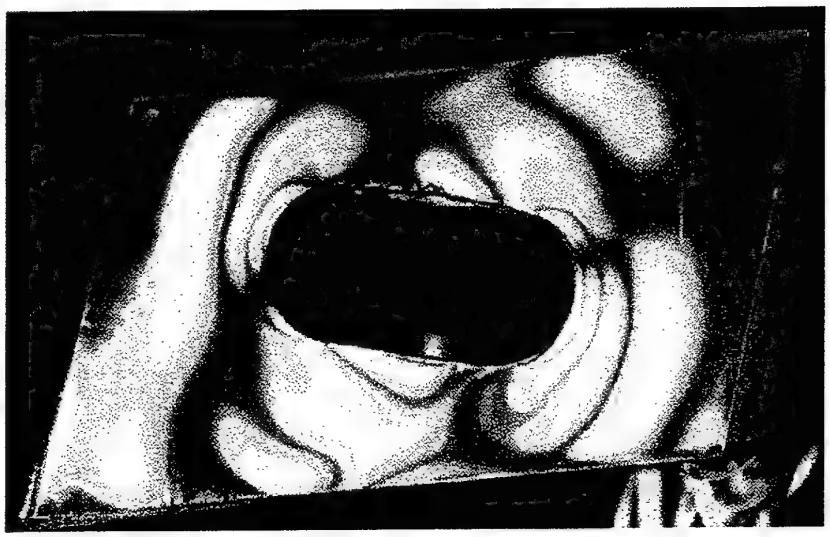

Figure 18. Photoelastic strain distribution at maximum interference-fitting level for Specimen 1.

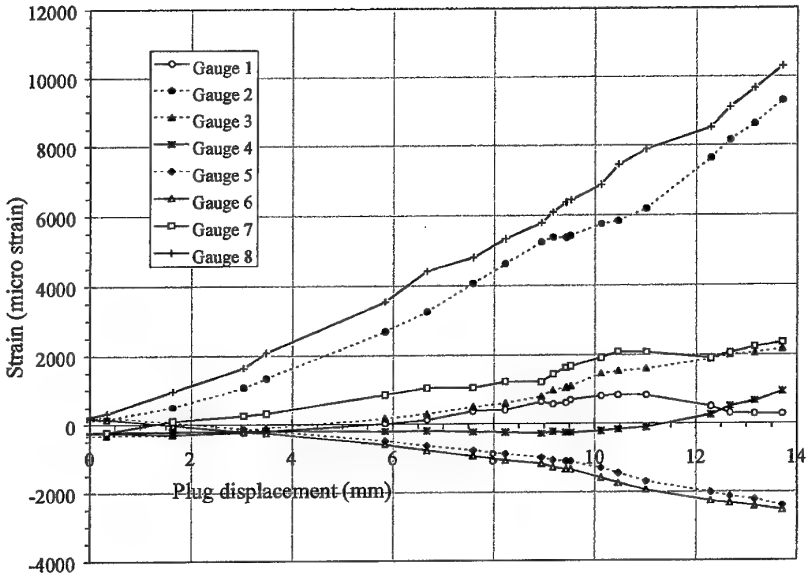

Figure 19. Strain response as a function of corrected plug displacement for Specimen 2, during the cold-expansion process.

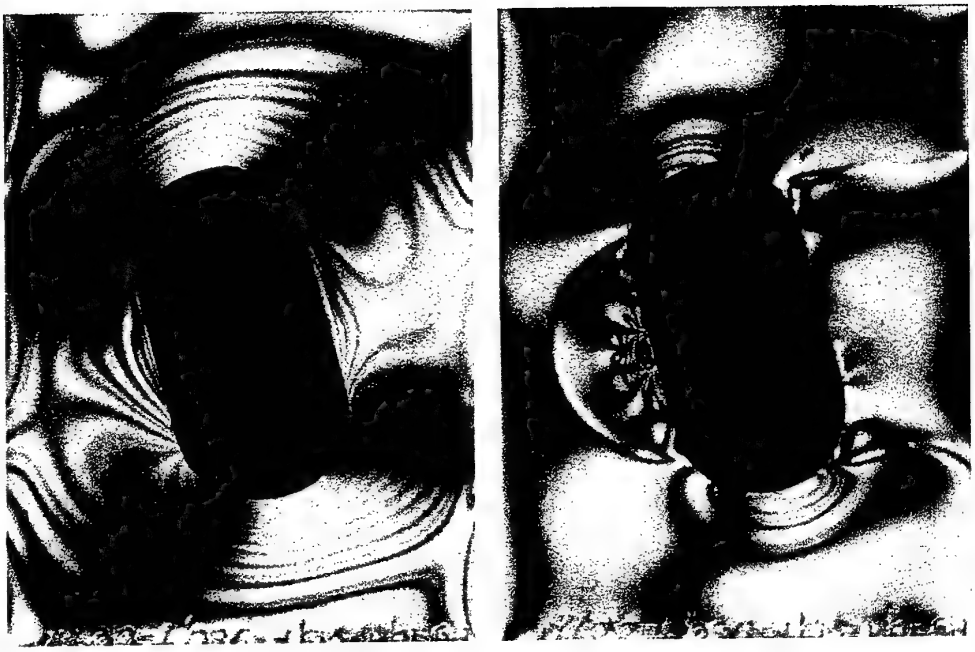

Figure 20. Photoelastic strain distributions for Specimen 2 at maximum cold expansion (left) and after cold expansion (right).

Figure 21. Stainless-steel sleeve used in the cold expansion of Specimen 2, showing the extent of cracking (original manufactured slit at middle left).

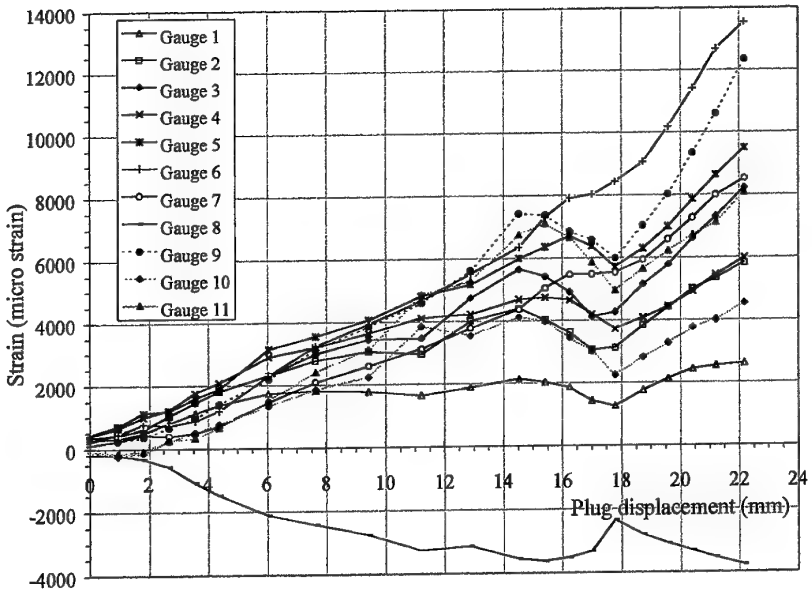

Figure 22. Strain response as a function of corrected plug displacement for Specimen 3 during the cold-expansion process.

Figure 23. Photoelastic strain distributions for Specimen 3 at maximum cold expansion (left) and after cold expansion (right).

Figure 24. Cracked cold-expansion plug after testing of Specimen 1.

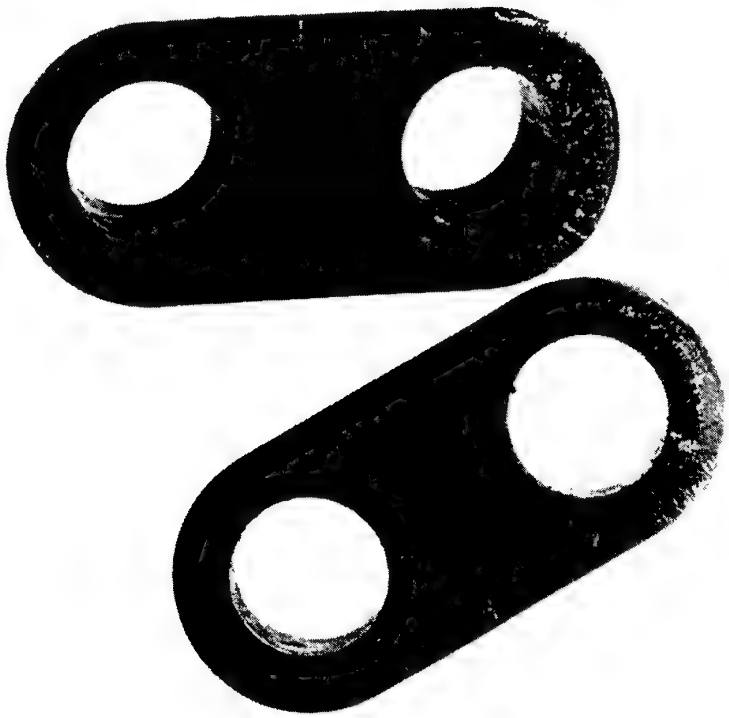

Figure 25. Broken cold-expansion plug after testing of Specimen 2.

Table 1: Estimated thickness of adhesive layer for different photoelastic coating cases, for Specimen 1 with plate thickness of 5.13 mm.

Photoelastic coating thickness (mm)	Total thickness of plate and bonded coating (mm)	Estimated adhesive layer thickness (mm)
2.0	7.22	0.09
1.0	6.32	0.19
0.5	5.76	0.13
0.25	5.50	0.12

Table 2: Strain-gauge readings for gauges 1 to 9 on Specimen 1 during the cold-expansion process.

		Strain readings								
Plug assembly length (mm)	Plug disp. (mm)	Gauge 1 (με)	Gauge 2 (με)	Gauge 3 (με)	Gauge 4 (με)	Gauge 5 (με)	Gauge 6 (με)	Gauge 7 (με)	Gauge 8 (με)	Gauge 9 (με)
(no plug)	(no plug)	-0.3847	-4.9455	-4.072	-4.425	-1.7039	-0.7814	1.0316	1.994	1.7639
70.15	-1.2	1.6563	13.164	5.7145	47.826	-13.165	-42.256	6.2317	0.99081	5.0998
68.74	0.21	14.453	104.75	-19.722	397.83	-12.228	-42.275	-39.93	1.6306	-181.32
68.15	0.80	19.938	173.13	-43.794	631.95	25.509	-40.791	-86.314	12.862	-413.9
67.48	1.47	16.978	356.74	-90.959	927.48	-153.6	581.05	-464.31	-109.08	-1445.9
65.93	3.02	46.898	896.64	-680.42	2281.8	-501.31	1459.2	-952.22	-501.05	-2616.7
65.11	3.84	52.609	1033.1	-965.24	2618	-551.77	1769	-1191.3	-767.88	-2800
64.57	4.38	57.282	1151	-1218	2963.3	-664.55	2150.4	-1439.5	-1007.7	-2966.8
64.15	4.80	62.999	1370.2	-1514.4	3427.6	-951.82	2645.8	-1732.5	-1074	-3049.7
63.7	5.25	64.168	1450.8	-1670.8	3637.1	-1043	2951	-1940.1	-1241.3	-3171.9
63.09	5.86	76.815	1551.1	-1953.1	3930.5	-1238.1	3463.6	-2002.1	-1423.4	-3171.7
62.35	6.60	82.48	1611	-2136.7	4137.5	-1293	3948.6	-2259.8	-1814.6	-3293
62.02	6.93	82.954	1675.7	-2239.1	4301.6	-1391.9	4295.9	-2457.7	-1991.9	-3383.6
61.72	7.23	83.224	1779.5	-2381.4	4539.9	-1609.3	4832.3	-2786.4	-2122	-3481
59.98	8.97	120.27	2734.7	-3761.3	7417.7	-2879.1	7265.9	-3816.2	-2358.1	-3621.4
56.84	12.11	138.94	3242.3	-6186.8	10789	-4683	11355	-4879.2	-2843.5	-3622.7
55.59	13.36	128.9	3252.2	-7160.7	11920	-5558.1	13101	-5510.4	-3127.2	-3820.7
54.35	14.60	130.03	3332.3	-8004.9	13195	-6811.3	15300	-6439.8	-3377.5	-3905.3
52.72	16.23	109.56	3176.8	-10581	22917	-10255	16338	-6701.6	-3460.3	-4007.1
52.12	16.83	99.18	3059.6	-10950	23181	-10402	16447	-6764.6	-3600.7	-3995.1
51.29	17.66	88.825	3191.1	-11287	24837	-11036	17579	-6850.6	-3530.6	-3932.8
(no plug)	-	-28	-256	-4733	13150	-6004	7280	-1184	49	-92

Table 3: Strain-gauge readings for gauges 10 to 18 on Specimen 1 during the cold-expansion process.

		Strain readings								
Plug assembly length (mm)	Plug disp. (mm)	Gauge 10 (με)	Gauge 11 (με)	Gauge 12 (με)	Gauge 13 (με)	Gauge 14 (με)	Gauge 15 (με)	Gauge 16 (με)	Gauge 17 (με)	Gauge 18 (με)
(no plug)	(no plug)	0.80015	1.9251	-0.428	-0.5733	-1.4646	-0.6117	0.14746	-0.2895	-1.0775
70.15	-1.2	-7.0565	-10.288	-9.5994	-8.3384	-100.78	16.096	21.336	5.8808	6.3727
68.74	0.21	-13.576	72.189	-110.28	148.05	-733.58	238.06	186.13	4.4002	29.512
68.15	0.8	-93.968	353.25	-553.47	532.59	-1224.7	561.33	374.61	1.022	45.067
67.48	1.47	-256.52	621.39	-777.15	613.16	-1306.8	531.63	295.39	20.884	30.419
65.93	3.02	-498.27	1225.8	-1551.5	1431.1	-2338.6	1471.1	750.79	5.8947	48.345
65.11	3.84	-612.05	1728	-2079.4	1935.8	-2880	1921.3	973.27	1.8736	60.614
64.57	4.38	-726.84	2176.7	-2481.8	2246.2	-3263.9	2320.7	1155.4	5.2571	68.152
64.15	4.8	-748.51	2205.2	-2464.2	2308.4	-3231.0	2321.6	1094.4	4.7294	51.542
63.7	5.25	-827.27	2513.1	-2750.4	2518.7	-3450.0	2492.3	1158.6	8.8194	52.674
63.09	5.86	-900.53	2832.4	-3268.7	2966.2	-4072.5	3080.9	1490.1	-18.352	48.92
62.35	6.6	-1037.3	3342.9	-3935.3	3557.9	-4986.0	3596.8	1762.4	-27.25	56.585
62.02	6.93	-1101	3555.2	-4215.2	3752.4	-5247.7	3689.9	1793.8	-17.814	61.876
61.72	7.23	-1147.9	3676.3	-4349.9	3842.5	-5340.4	3638.6	1715.3	-11.997	51.784
59.98	8.97	-1298	3985.1	-4942.6	4442.6	-6903.2	3883.8	1681.9	-24.864	21.349
56.84	12.11	-2051.9	8277.5	-10826	7097.6	-11522	4849.7	2053.1	-25.553	60.595
55.59	13.36	-2290.4	9657.9	-12809	7963.7	-12035	5109.6	2037.9	-13.659	72.345
54.35	14.6	-2440.3	11259	-14970	9072.1	-13581	5452	2014.5	-6.2462	88.613
52.72	16.23	-2773.9	13009	-17053	10193	-14768	5113.1	1434.3	113.65	32.969
52.12	16.83	-2724.2	14270	-18243	10939	-16069	5540.7	1613.9	100.2	68.523
51.29	17.66	-2559.3	13658	-18002	12478	-16517	4851.8	1064.9	121.27	96.903
(no plug)	-	-12	5966	-10577	5270	-9060	-356	-772	31	84

Table 4: Peak and residual strains for Specimen 1 during and after the cold-expansion process.

Strain gauge number	Approx.angular position of gauge as defined in Fig. 10 (degrees)	Orientation of gauge	Peak strain (με)	Residual strain (με)
	Curved section (θ)			
2	180t	hoop	3332	-256
3	157.5t	radial	-11287	-4733
4	135t	hoop	24837	13150
5	90t (r=4 mm)	radial	-11036	-6004
6	45t	hoop	17579	7280
7	22.5t	radial	-6851	-1184
8	0t	radial	-3601	49
10	180b	radial	-2774	-12
11	157.5b	hoop	14270	5966
12	135b	radial	-18243	-10577
13	90b (r=4 mm)	hoop	12478	5270
14	45b	radial	-16517	-9060
15	22.5b	hoop	5541	-356
16	0b	hoop	2053	-772
	Straight section (α)			
1	180	hoop	139	-28
9	0	radial	-4007	-92
17	n/a (remote)	n/a (remote)	121	31
18	n/a (remote)	n/a (remote)	97	84

Table 5: Strain-gauge readings for gauges 1 to 9 on Specimen 1 during the interference-fitting process.

Plug assembly length (mm)	Plug disp. (mm)	Strain readings Gauge 1 (με)	Gauge 2 (με)	Gauge 3 (με)	Gauge 4 (με)	Gauge 5 (με)	Gauge 6 (με)	Gauge 7 (με)	Gauge 8 (με)	Gauge 9 (με)
(no plug)	(no plug)	-0.47308	-4.6904	0.91704	2.2859	4.0574	-16.821	2.8547	-2.7386	6.1381
31.76	-0.11	1.1998	8.6951	0.8856	12.955	-7.8957	-20.678	1.3204	-9.7118	19.896
31.2	0.45	4.2026	0.0412	10.469	9.7935	19.224	-81.232	-132.91	-19.9	8.5962
30.26	1.39	16.886	23.452	29.493	-51.686	88.252	-214.64	-217.07	-70.108	-46.579
29.52	2.13	37.255	404.4	-200.28	597.87	-412.02	489.37	-900.21	-227.07	-96.018
28.52	3.13	69.45	397.55	-611.77	620.71	-238.14	362.1	-829.33	-559.65	-193.98
27.45	4.2	86.978	606.46	-989.97	1175.6	-476.48	818.76	-1132.7	-913.17	-255.36
26.38	5.27	88.307	816.47	-1355.9	1650.1	-643.36	1244	-1519.9	-1194.2	-317.16
25.75	5.9	97.41	1193.7	-1936.7	2343.6	-1044.4	1831.3	-1947.1	-1301.2	-334.04
24.75	6.9	81.96	1078.2	-1899.2	2389.8	-825.24	1800.3	-2070.2	-1693.6	-452.24
23.68	7.97	74.488	1206.5	-2304.4	2900.7	-889.37	2002.4	-2141.3	-1880.4	-522.94

Table 6: Strain-gauge readings for gauges 10 to 18 on Specimen 1 during the interference-fitting process.

Plug Assembly Length (mm)	Plug disp. (mm)	Strain readings Gauge 10 (με)	Gauge 11 (με)	Gauge 12 (με)	Gauge 13 (με)	Gauge 14 (με)	Gauge 15 (με)	Gauge 16 (με)	Gauge 17 (με)	Gauge 18 (με)
(no plug)	(no plug)	-1.1817	-3.0427	-10.612	8.7413	0.72106	-8.4094	-2.0004	-4.3487	-2.8501
31.76	-0.11	-7.8557	32.154	4.5309	14.67	9.1259	-0.63387	16.398	1.2835	-4.2653
31.2	0.45	-43.62	180.47	-22.626	44.427	46.639	0.94294	50.111	8.2403	-10.506
30.26	1.39	-121.83	670.86	-288.81	275.81	-454.15	134.54	256.14	14.796	-5.5629
29.52	2.13	-99.664	595.2	-57.193	121.3	-469.55	6.8598	272.23	10.885	-35.613
28.52	3.13	-276.51	1414.7	-877.38	786.15	-1780.8	745.1	649.57	-1.1122	-13.911
27.45	4.2	-442.88	1896.7	-1486.8	1261.1	-2301	1189.2	858.91	-9.0128	-0.49472
26.38	5.27	-644.39	2267.1	-1959.5	1650.1	-2603.6	1540.3	928.46	-5.1813	35.521
25.75	5.9	-794.34	2195.6	-1862.9	1729.8	-2570.7	1561.8	820.24	-8.548	34.518
24.75	6.9	-1087.9	2765.5	-2444.8	2163	-3065.5	2051.9	957.84	-5.4396	100.13
23.68	7.97	-1331.4	3099.1	-2715.6	2559	-3387.2	2481.2	1017.4	-17.168	142.23

Table 7: Peak strains for Specimen 1 during the interference-fitting process.

Strain gauge Number	Approx. angular position of gauge as defined in Fig. 10 (degrees)	Orientation of gauge	Peak strain (με)
	Curved section (θ)		
2	180t	hoop	1207
3	157.5t	radial	-2304
4	135t	hoop	2901
5	90t (r=4 mm)	radial	-1044
6	45t	hoop	2002
7	22.5t	radial	-2141
8	0t	radial	-1880
10	180b	radial	-1331
11	157.5b	hoop	3099
12	135b	radial	-2716
13	90b (r=4 mm)	hoop	2559
14	45b	radial	-3387
15	22.5b	hoop	2481
16	0b	hoop	1017
	Straight section (α)		
1	180	hoop	97
9	0	radial	-523
17	n/a (remote)	n/a (remote)	-17
18	n/a (remote)	n/a (remote)	142

Table 8: Strain-gauge readings for Specimen 2 during the cold-expansion process.

Plug assembly length (mm)	Plug disp. (mm)	Strain readings Gauge 1 (με)	Gauge 2 (με)	Gauge 3 (με)	Gauge 4 (με)	Gauge 5 (με)	Gauge 6 (με)	Gauge 7 (με)	Gauge 8 (με)
(no plug)	(no plug)	-474.52	-304.56	-416.86	-377.39	279.12	257.15	-376.3	-216.38
68.71	-2.71	-352.86	-257.63	-352.51	-263.89	249.93	239.61	-303.69	-211.68
66.96	-0.96	-253.31	8.3004	-346.07	-257.54	261.83	230.2	-352.95	-55.909
65.66	0.34	-254.47	152.44	-327.13	-241.26	202.66	140.4	-234.25	313.72
64.35	1.65	-306.73	502.98	-312.5	-221.98	54.401	-32.685	88.794	965.66
62.95	3.05	-237.89	1063.4	-161.36	-195.5	-131.62	-214.45	255.22	1639.5
62.5	3.50	-193.4	1335.9	-99.772	-183.2	-177.59	-253.94	315.1	2081.4
60.15	5.85	15.892	2685.2	160.85	-209.32	-486.36	-593.9	851.68	3539.1
59.32	6.68	115.24	3247	292.09	-200.29	-629.66	-771.8	1041.8	4403.2
58.4	7.60	367.75	4061.7	495.42	-240.99	-774.5	-940.49	1052	4794.3
57.76	8.24	402.65	4612.8	593.75	-248.34	-879.31	-1069.7	1221.9	5332
57.05	8.95	635.69	5239.5	790.63	-291.9	-987	-1164.4	1212.6	5782.1
56.82	9.18	570.07	5374	971.34	-232.23	-1068.8	-1272.2	1429.7	6085.1
56.56	9.44	608.68	5364	1046.3	-264.24	-1101.4	-1334.2	1624.6	6367.6
56.47	9.53	694.77	5414	1087.4	-263.45	-1102.8	-1342.5	1662.6	6431.6
55.87	10.13	796.5	5747.5	1450.4	-219.15	-1297.2	-1583.7	1904.8	6864.9
55.53	10.47	828.07	5835.6	1513.6	-172.09	-1443.5	-1746.5	2089.3	7441.4
54.98	11.02	820.66	6184.3	1586.8	-119.31	-1696.1	-1939.8	2063.4	7878.8
53.7	12.30	491.94	7632	1865.7	251.06	-2016.4	-2268.5	1889.8	8515.6
53.32	12.68	300.18	8151.6	1983.7	499.78	-2128.6	-2326.2	2044.6	9095.7
52.83	13.17	279.78	8619.5	2045.8	652.8	-2223.8	-2420.2	2222.9	9649.3
52.28	13.72	274.44	9291.7	2161.8	921.86	-2397.6	-2536.5	2344.1	10294
(no plug)	-	155.24	1697.6	453.13	353.33	-109.65	-305.49	26.116	2018.7

Table 9: Peak and residual strains for Specimen 2 during and after the cold-expansion process.

Strain gauge number	Approx. angular position of gauge as defined in Fig. 10 (degrees)	Orientation of gauge	Peak strain (με)	Residual strain (με)
	Curved section (θ)			
1	0t	hoop	828	155
2	90t	hoop	9292	1698
3	180t	hoop	2162	453
6	0b	radial	-2537	-305
7	0b	hoop	2344	26
8	90b	hoop	10294	2019
	Straight section (α)			
4	180	hoop	922	353
5	180	radial	-2398	-110

Table 10: Strain-gauge readings for Specimen 3 during the cold-expansion process.

		Strain readings										
Plug assembly Length (mm)	Plug disp. (mm)	Gauge 1 (με)	Gauge 2 (με)	Gauge 3 (με)	Gauge 4 (με)	Gauge 5 (με)	Gauge 6 (με)	Gauge 7 (με)	Gauge 8 (με)	Gauge 9 (με)	Gauge 10 (με)	Gauge 11 (με)
67.85	-0.85	230	278	264	202	185	21	3	-173	32	-5	-16
66.05	0.95	318	409	424	645	704	448	230	-209	230	-242	-181
65.19	1.81	492	600	583	992	1117	750	422	-332	349	-147	-89
64.32	2.68	796	1023	1021	1213	1193	723	395	-589	653	233	260
63.43	3.57	1111	1461	1451	1758	1591	863	477	-1095	950	494	322
62.62	4.38	1372	1803	1797	2085	1875	1174	695	-1481	1408	757	654
60.95	6.05	1737	2302	2310	2903	3148	2292	1457	-2114	2180	1327	1494
59.35	7.65	1798	2773	2983	3200	3553	3250	2087	-2435	3143	1843	2400
57.56	9.44	1768	3050	3435	3627	4060	3916	2588	-2755	3854	2236	3117
55.77	11.23	1636	2955	3462	4112	4810	4662	3114	-3259	4582	3846	4832
54.10	12.90	1873	4005	4747	4217	5173	5520	3768	-3145	5615	3526	5280
52.46	14.54	2131	4383	5642	4682	5988	6347	4360	-3554	7415	4108	6747
51.57	15.43	2011	4017	5410	4734	6346	7297	5041	-3634	7364	3984	7102
50.74	16.26	1848	3615	4908	4652	6693	7905	5470	-3514	6839	3445	6650
49.98	17.02	1421	3047	4105	4195	6378	8026	5473	-3329	6573	3004	5863
49.20	17.80	1250	3114	4251	3719	5707	8417	5529	-2357	5992	2237	4962
48.25	18.75	1746	3824	5154	4080	6287	9058	5930	-2814	7025	2809	5643
47.40	19.60	2106	4407	5777	4433	6991	10164	6576	-3097	8021	3267	6209
46.57	20.43	2417	4994	6612	4909	7853	11408	7261	-3316	9333	3755	6722
45.78	21.22	2520	5343	7302	5433	8627	12675	7990	-3536	10583	3999	7118
44.81	22.19	2605	5814	8215	5976	9481	13539	8504	-3773	12333	4533	8068
(no plug)	-	-342	-106	786	-154	1273	3236	1642	16	2440	-412	848

Table 11: Peak and residual strains for Specimen 3 during and after the cold-expansion process.

Strain gauge number	Angular position of gauge as defined in Fig. 10 (degrees)	Orientation of gauge	Peak strain (με)	Residual strain (με)
	Curved section (θ)			
1	180t	hoop	2605	-342
2	157.5t	hoop	5814	-106
3	135t	hoop	8215	786
4	157.5b	hoop	5976	-154
5	135b	hoop	9481	1273
6	90b	hoop	13539	3236
7	90b (r=4.0)	hoop	8504	1642
8	180b	radial	-3773	16
9	90t	hoop	12333	2440
10	22.5t	hoop	4533	-412
11	45t	hoop	8068	848

Table 12: Comparison of peak strain results for Specimens 1, 2 and 3, measured during the cold-expansion process, including the maximum level of cold expansion (CX).

Approx. angular position of gauge as defined in Fig. 10 (degrees)	Orientation of gauge	Specimen 1 2.78% CX Peak strain (με)	Gauge number	Specimen 2 2.16% CX Peak strain (με)	Gauge number	Specimen 3 3.49% CX Peak strain (με)	Gauge number
Curved section (θ)							
0	hoop	2053	16	2344	7		
				828	1		
	radial	-3601	8	-2537	6		
22.5	hoop	5541	15			4533	10
45	hoop	17579	6			8068	11
90	hoop			9292	2	12333	9
				10294	8	13539	6
90 (r=4)	hoop	12478	13			8504	7
135	hoop	24837	4			8215	3
						9681	5
157.5	hoop	14270	11			5976	4
						5814	2
180	hoop	3332	2	2162	3	2605	1
	radial	-2774	10			-3773	8
Straight section (α)							
180	hoop	139	1	922	4		

Table 13: Comparison of residual strain results for Specimens 1, 2 and 3, measured at the completion of the cold-expansion process, including the maximum level of cold expansion (CX).

Approx. angular position of gauge as defined in Fig. 10 (degrees)	Orientation of gauge	Specimen 1 2.78% CX		Specimen 2 2.16% CX		Specimen 3 3.49% CX	
		Residual strain (με)	Gauge number	Residual strain (με)	Gauge number	Residual strain (με)	Gauge number
Curved section (θ)							
0	hoop	-772	16	26	7		
				155	1		
	radial	49	8	-305	6		
22.5	hoop	-356	15			-412	10
45	hoop	7280	6			848	11
90	hoop			1698	2	2440	9
				2019	8	3236	6
90 (r=4)	hoop	5270	13			1642	7
135	hoop	13150	4			786	3
						1273	5
157.5	hoop	5966	11			-154	4
						-106	2
180	hoop	-256	2	453	3	-342	1
	radial	-12	10			16	8
Straight section (α)							
180	hoop	-28	1	353	4		

DISTRIBUTION LIST

Cold Expansion Tests for Plates Containing Elongated Holes

M. Heller, R. L. Evans and R. B. Allan

AUSTRALIA

DEFENCE ORGANISATION

Task Sponsor
AIR OIC ASI-DGTA

S&T Program
Chief Defence Scientist
FAS Science Policy
AS Science Corporate Management
} shared copy
Director General Science Policy Development
Counsellor Defence Science, London (Doc Data Sheet)
Counsellor Defence Science, Washington (Doc Data Sheet)
Scientific Adviser to MRDC Thailand (Doc Data Sheet)
Scientific Adviser Policy and Command
Navy Scientific Adviser (Doc Data Sheet and distribution list only)
Scientific Adviser - Army (Doc Data Sheet and distribution list only)
Air Force Scientific Adviser
Director Trials

Aeronautical and Maritime Research Laboratory
Director

Chief of Airframes and Engines Division
Research Leader Fracture Mechanics
Research Leader Aerospace Composite Structures
Research Leader Structural Integrity
K. Watters
G. Clark
D. Graham
I. Anderson
P. White
K. Walker
P. Piperias
M. Heller (10 copies)
R. Evans (2 copies)

DSTO Library and Archives
Library Fishermans Bend
Library Maribyrnong
Library Salisbury (2 copies)
Australian Archives
Library, MOD, Pyrmont (Doc Data sheet only)
*US Defense Technical Information Center, 2 copies

*UK Defence Research Information Centre, 2 copies
*Canada Defence Scientific Information Service, 1 copy
*NZ Defence Information Centre, 1 copy
National Library of Australia, 1 copy

Capability Development Division
Director General Maritime Development (Doc Data Sheet only)
Director General Land Development (Doc Data Sheet only)
Director General C3I Development (Doc Data Sheet only)
Director General Aerospace Development

Navy
SO (Science), Director of Naval Warfare, Maritime Headquarters Annex, Garden Island, NSW 2000. (Doc Data Sheet only)

Army
ABCA Standardisation Officer, Puckapunyal, (4 copies)
SO (Science), DJFHQ(L), MILPO Enoggera, Queensland 4051 (Doc Data Sheet only)
NAPOC QWG Engineer NBCD c/- DENGRS-A, HQ Engineer Centre Liverpool Military Area, NSW 2174 (Doc Data Sheet only)

Air Force
CENG 501 WING, AMBERLEY
OIC ATF ATS, RAAFSTT, WAGGA (2 copies)

Intelligence Program
DGSTA Defence Intelligence Organisation
Defence Intelligence Organisation-Information Centre

Corporate Support Program
OIC TRS, Defence Regional Library, Canberra

UNIVERSITIES AND COLLEGES
Australian Defence Force Academy
Library
Head of Aerospace and Mechanical Engineering
Serials Section (M list), Deakin University Library, Geelong, 3217
Senior Librarian, Hargrave Library, Monash University
Librarian, Flinders University

OTHER ORGANISATIONS

NASA (Canberra)
AGPS

OUTSIDE AUSTRALIA

ABSTRACTING AND INFORMATION ORGANISATIONS

Library, Chemical Abstracts Reference Service
Engineering Societies Library, US
Materials Information, Cambridge Scientific Abstracts, US
Documents Librarian, The Center for Research Libraries, US

INFORMATION EXCHANGE AGREEMENT PARTNERS

Acquisitions Unit, Science Reference and Information Service, UK
Library - Exchange Desk, National Institute of Standards and Technology, US
National Aerospace Laboratory, Japan (
National Aerospace Laboratory, Netherlands

SPARES (5 copies)

Total number of copies: **72**

DEFENCE SCIENCE AND TECHNOLOGY ORGANISATION
DOCUMENT CONTROL DATA

1. PRIVACY MARKING/CAVEAT (OF DOCUMENT)

2. TITLE

Cold Expansion Tests for Plates Containing Elongated Holes

3. SECURITY CLASSIFICATION (FOR UNCLASSIFIED REPORTS THAT ARE LIMITED RELEASE USE (L) NEXT TO DOCUMENT CLASSIFICATION)

Document ... (U)
Title (U)
Abstract (U)

4. AUTHOR(S)

M. Heller, R. L. Evans and R. B. Allan

5. CORPORATE AUTHOR

Aeronautical and Maritime Research Laboratory
PO Box 4331
Melbourne Vic 3001 Australia

6a. DSTO NUMBER	6b. AR NUMBER	6c. TYPE OF REPORT	7. DOCUMENT DATE
DSTO-TN-0233	AR-011-113	Technical Note	October 1999

8. FILE NUMBER	9. TASK NUMBER	10. TASK SPONSOR	11. NO. OF PAGES	12. NO. OF REFERENCES
M1/9/318	AIR 98/220	AIR OIC ASI-DGTA	33	8

13. DOWNGRADING/DELIMITING INSTRUCTIONS

14. RELEASE AUTHORITY

Chief, Airframes and Engines Division

15. SECONDARY RELEASE STATEMENT OF THIS DOCUMENT

Approved for public release

OVERSEAS ENQUIRIES OUTSIDE STATED LIMITATIONS SHOULD BE REFERRED THROUGH DOCUMENT EXCHANGE, PO BOX 1500, SALISBURY, SA 5108

16. DELIBERATE ANNOUNCEMENT

No Limitations

17. CASUAL ANNOUNCEMENT Yes

18. DEFTEST DESCRIPTORS

Fatigue life; F-111C wing pivot fittings; Holes (openings); Cold working; Interference fit devices; Expansion

19. ABSTRACT

Cold-expansion testing of D6ac plates containing an elongated (non-circular) hole, of 2:1 aspect ratio, has been undertaken using an AMRL designed interference fit plug/sleeve arrangement. The aim has been to determine the practical viability of the process as an option for addressing the cracking problem at the non-circular fuel flow vent hole number 13 in the wing pivot fitting of the F-111C aircraft in service with the RAAF. The key issue being that in the open literature, only cold expansion to circular holes has been reported, and application to non-circular holes would represent a significant new development. In the testing, three nominally identical plate specimens were cold expanded, with sleeves of two different material types (ie high strength tool steel (D2) and stainless steel) being assessed. Strain gauge readings around the elongated hole boundary were recorded at various stages of the cold-expansion process, as well as some typical full-field qualitative photoelastic strain distributions. In all cases nominal expansion levels greater than 2.5% were achieved, along with maximum peak strains of more than 10,000 micro-strain and maximum residual strains greater than 1600 micro-strain. These results indicate that highly effective cold expansion has been achieved. It was also demonstrated that subsequent to cold expansion, effective interference fitting could be achieved, without the need for post cold-expansion machining. The particular advantages available by using stainless steel sleeves have been identified, and an improved surface finish at the holes in the plug is also recommended. Fatigue testing of the existing design, (with minor amendments) is now proposed to confirm its anticipated suitability as an effective fatigue life extension option.